Molecular Crystals and Liquid Crystals

Publication details, including instructions for authors and subscription information:
http://www.tandfonline.com/loi/gmcl20

HEDGEHOG ANNIHILATION IN A CONFINED NEMATIC LIQUID CRYSTAL

M. Svetec [a] , Z. Brada[cbreve] [a] , S. Kralj [a b] & S. [Zbreve]umer [b c]

[a] Laboratory of Physics of Complex Systems, Faculty of Education, University of Maribor, Koro[sbreve]ka 160, 2000 Maribor, Slovenia

[b] Jo[zbreve]ef Stefan Institute, Jamova 39, 1000 Ljubljana, Slovenia

[c] Department of Physics, Faculty of Mathematics and Physics, University of Ljubljana, Jadranska 19, 1000 Ljubljana, Slovenia

Version of record first published: 07 Jan 2010

To cite this article: M. Svetec, Z. Brada[cbreve], S. Kralj & S. [Zbreve]umer (2004): HEDGEHOG ANNIHILATION IN A CONFINED NEMATIC LIQUID CRYSTAL, Molecular Crystals and Liquid Crystals, 413:1, 43-51

To link to this article: http://dx.doi.org/10.1080/15421400490432551

Mol. Cryst. Liq. Cryst., Vol. 413, pp. 43/[2179]–51/[2187], 2004

ISSN: 1542-1406 print/1563-5287 online
DOI: 10.1080/15421400490432551

HEDGEHOG ANNIHILATION IN A CONFINED NEMATIC LIQUID CRYSTAL

M. Svetec and Z. Bradač
Laboratory of Physics of Complex Systems, Faculty of Education, University of Maribor, Koroška 160, 2000 Maribor, Slovenia

S. Kralj
Laboratory of Physics of Complex Systems, Faculty of Education, University of Maribor, Koroška 160, 2000 Maribor, Slovenia
and
Jožef Stefan Institute, Jamova 39, 1000 Ljubljana, Slovenia

S. Žumer
Jožef Stefan Institute, Jamova 39, 1000 Ljubljana, Slovenia
and
Department of Physics, Faculty of Mathematics and Physics, University of Ljubljana, Jadranska 19, 1000 Ljubljana, Slovenia

Annihilation of a pair of nematic point defects, having opposite strength is studied numerically. The defects are enclosed within an infinite cylindrical cavity whose lateral wall enforces strong homeotropic anchoring. The Lebwohl-Lasher lattice model is used. The dynamics of the system consisting of $N > 10^5$ molecules is studied using the Brownian molecular dynamics. We study pre-collision, collision and post-collision regimes. In the first regime the defects are well separated and are clearly distinguishable. Latter the core structures of defects strongly overlap and gradually decay into the defectless state.

Keywords: annihilation; nematic liquid crystal; nucleation; point defects

This research was supported by the ESF network project COSLAB and Slovenian Office of Science (PO-0524-0106).

Address correspondence to M. Svetec, Laboratory of Physics of Complex Systems, Faculty of Education, University of Maribor, Koroška 160, 2000 Maribor, Slovenia.

I. INTRODUCTION

Defects in nematic liquid crystals (LCs) correspond to points or lines where the nematic director field $\vec{n}(\vec{r})$ is not uniquely defined [1,2]. To describe the core of a defect, where the nematic ordering is strongly distorted, additional degrees of nematic ordering have to be introduced [3,4,5]. In the core of a defect order is depressed and partially biaxial depending on temperature and the relative strength of nematic elastic constants [5,6,7]. The size of the core is roughly given by the relevant nematic (uniaxial or biaxial) order parameter correlation length ξ [7]. An important quantity characterising the symmetry of a defect is the winding strength (also called the Frank index M) [1,8]. It counts the number of rotations of $\vec{n}(\vec{r})$ on encircling the defect origin counter-clockwise.

In this study we focus to the annihilation of two nematic point defects (also called hedgehogs) with $M = 1$ (monopole) and $M = -1$ (antimonopole), respectively in a cylindrically confined nematic LC phase. The annihilation of a nematic monopole and antimonopole consists of the *pre-collision*, *collision* and *post-collision* regime (9). In the pre-collision regime defects are well separated with respect to ξ. The interaction between them is mediated via $\vec{n}(\vec{r})$ which can also strongly depend on the confining geometry and boundary conditions. This regime has already been studied both theoretically and experimentally [10–14]. In the collision and post-collision regime the cores of defects strongly overlap and the defects become gradually indistinguishable. This regime, which is the focus of this article, is governed by nematic order parameter and has not yet been studied.

The plan of the article is as follows. In Sec.II we describe the model we use. The results are presented in Sec.III and in the last section we summarise the results.

II. MODEL

II.1 Semi-microscopic Approach

In our simulation a pair of rod like LC *molecules* interacts via a simple pairwise Lebwohl-Lasher [15,16] potential

$$V_{ij} = -\frac{J}{r^6}(\vec{e}_i \cdot \vec{e}_j)^2. \tag{1}$$

Here the positive constant J measures the strength of the coupling tending to enforce parallel orientation of *molecules* located at $\vec{r}_i$ and $\vec{r}_j$ and pointing along unit vectors $\vec{e}_i$ and $\vec{e}_j$ respectively. $r = |\vec{r}_i - \vec{r}_j|$ is a relative separation of interacting *molecules* residing in a hexagonal lattice

with the characteristic lattice length a_0. A *molecule* in our model corresponds to a cluster of strongly interacted real molecules [16]. The interaction energy W_{int} of the whole sample is given as a sum over all pair interactions. The range of interaction is restricted to a sphere of radius $2a_0$.

This model yields in the standard elastic "director-field" $\vec{n}(\vec{r})$ continuum representation the approximation of equal Frank elastic constants [17,18]. The nematic director field at the i-th lattice site can be obtained as $\vec{n}(\vec{r}_i) = \langle \vec{e}_i \rangle$, where $\langle \ldots \rangle$ stands for the average over fast molecular motions (with respect to the sampling time used in an experimental observation) and small volume allocated to the point $\vec{r}_i$ taking into account head to tail invariance $\vec{e}_i = -\vec{e}_i$.

In our study the nematic LC phase is confined to a cylindrical cavity of radius $R = N_r a_0$ and length $L = N_z a_0$. The integers $2N_r$ and N_z are in our simulations typically varied in the range from 30 to 80. The cylinder axis is set along the z-direction of the Cartesian coordinate system, whose axes (x, y, z) point along the unit vectors $(\vec{e}_x, \vec{e}_y, \vec{e}_z)$, respectively. The lateral cylinder wall enforces strong homeotropic anchoring (i.e. at the surface *molecules* are oriented along the surface normal). In the z direction we impose periodic boundary conditions simulating an infinite cylindrical cavity.

The local orientation of molecules is parameterised as

$$\vec{e} = \vec{e}_x \sin\theta \cos\phi + \vec{e}_y \sin\theta \sin\phi + \vec{e}_z \cos\theta. \tag{2}$$

The time evolution of the variational parameters θ and ϕ is followed using the Brownian Molecular Dynamics. For computational details we refer the reader to Refs. [19,20].

II.2 Director Structures

The equilibrium nematic director configuration of our system is the so-called *Escaped Radial* (ER) structure [21]. Its director field structure is shown in Figure 1a. In it $\vec{n}(\vec{r})$ gradually reorients from the radial orientation at the cylinder wall towards $+\vec{e}_z$ (or $-\vec{e}_z$) at the cylinder axis. We schematically indicate the ER-like structure by <<< and the structures with escapes along $+\vec{e}_z$ (>>>) and $-\vec{e}_z$ (<<<) are equivalent.

On cooling the liquid crystal from the high temperature isotropic (i.e. ordinary liquid) to the nematic phase domains of ER-like structures with alternative preference along $+\vec{e}_z$ and $-\vec{e}_z$ are expected to form due to the symmetry breaking (schematically: <<<><<<>>>). The domain collision sites give rise to nematic monopoles (collision sites >>><<<) and antimonopoles (collision sites <<<>>>). The corresponding structure is called the *escaped radial structure with point defects* (ERPD) [22] (Fig. 1b). This structure is metastable with respect to the ER. The

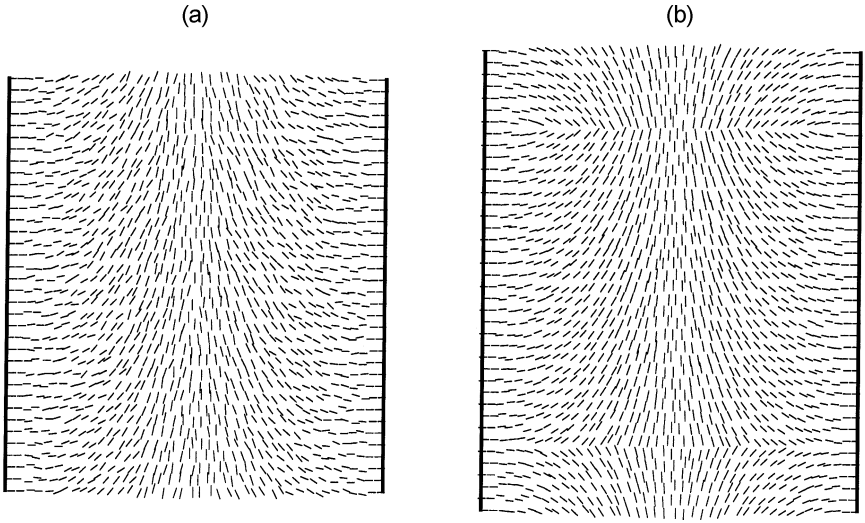

FIGURE 1 The (a) Escaped Radial (ER) and (b) Escaped Radial structure with Point Defects (ERPD) in the (x,z) plane. In ideal case the structures exhibit the cylindrical symmetry. The cylinder wall is denoted with heavy lines.

ERPD → ER transition can be realised continuously via annihilation of neighbouring monopole-antimonopole pairs. Note that in several experimental situations the defects of the ERPD structure are frozen if the distance between neighbouring defects is larger than 2 R [12,19]. For such distances the attractive force between defects is negligible small [12] and is overshadowed by thermal fluctuations or deviations from the topological and geometrical conditions described in our model.

III. RESULTS

We study annihilation of a pair of nematic point defects of strength $M = 1$ (monopole) and $M = -1$ (antimonopole) in a cylindrical cavity characterised by $2N_r$ and N_z which are typically varied between 30 and 80. Initially a pair of "point" defects is placed at the cylinder axis as shown in Figure 1b. This was achieved by enforcing 3 alternative ER-like domains (i.e. >>><<<>>>), using the analytic ansatz [18,19]. The starting separation $d = d_0$ of defects is large enough ($d_0/(2R) > 0.5$) so that initially the core structures of defects are essentially independent of each other. On the other hand d_0 is small enough ($d_0/(2R) < 1$) to drive the system into the defectless structure in a computationally accessible time (in approximately 10000 sweeps).

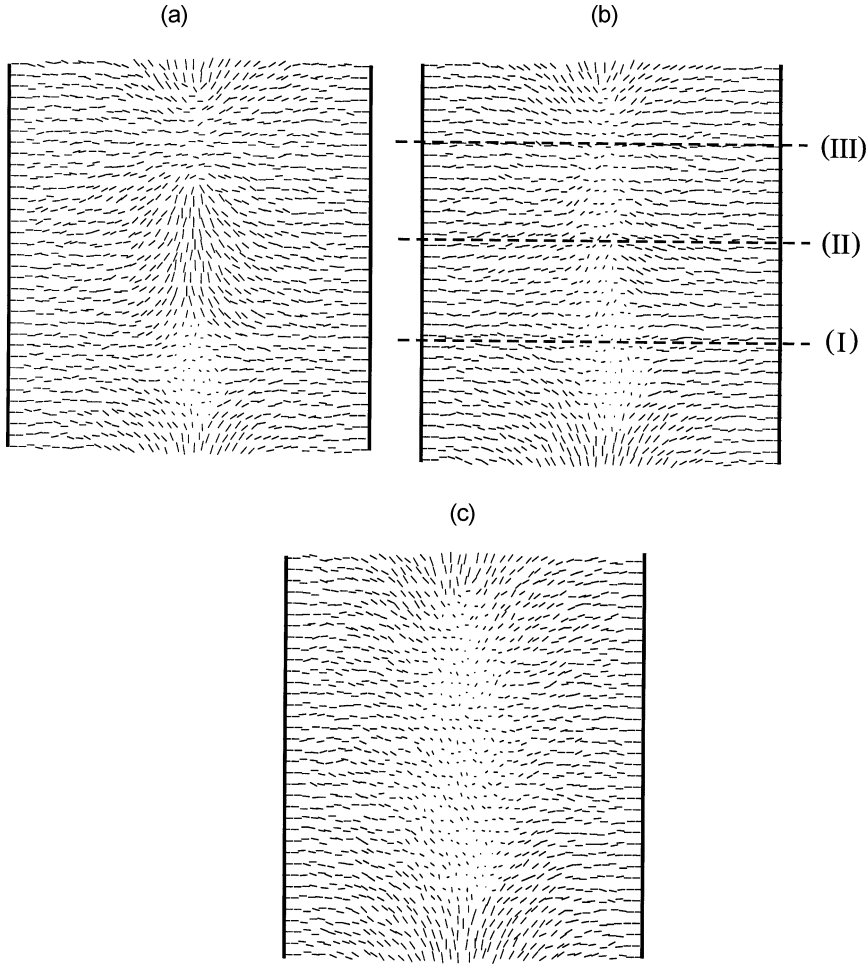

FIGURE 2 Different annihilation stages of a pair nematic monopole and antimonopole at N sweeps in the (x,z) plane. (a) N = 2000, the defects form a ring-like structure. (b) N = 2560, collided defects form a twisted single ring-like structure. The three dashed lines indicate slides, that are shown in (x,y) projection in Figure 3. (c) N = 2700, the two "rings" merge into a single "ring" lying predominantly in the (x,z) plane. In all figures $N_z = 70$, $2N_r = 34$, $d_0/R = 0.74$. A point in figures denotes a molecule pointing out of the paper.

Some stages of a typical annihilation scenario in the director field representation are shown in Figure 2 for $2N_r = 34$ and $N_z = 70$. In the initial structure we enforce "point" defects (see Fig. 1b). After some 1000 sweeps (Fig. 2a) the defects form a ring-like like structure [3,4,7].

In this structure the "centre" of defect is uniaxial and surrounded with a circular "ring", characterised by the ring radius ξ_r, at which strong elastic distortions are localised. For a detail structure of the ring in the continuum description we refer the reader to Refs. [4,7]. For well-separated defects the ring structures are essentially independent of each other [4] and thus soon (i.e. after 1000 sweeps) adopt the quasi-equilibrium defect core structure. For experimental observations this defect structure appears as a point because the "ring" radius ξ_r is comparable to the biaxial nematic order parameter correlation length ξ (< 30 nm) [4]. In our simulation the equilibrium "ring" radius is $\xi_{eq} \approx 7a_0$. The ring radia of both defects are the same within the numerical accuracy in accordance with continuum predictions [23]. Due to cylindrical confinement the "rings" after the creation tend to orient with their axes perpendicular to the cylinder axis (Fig. 2a) [24]. The two "rings" gradually approach and their axes slowly (on the time scale of 1000 sweeps) rotate due to thermal fluctuations. In the regime where $d > \xi_{eq}$ the "ring" radia do not vary within the experimental error. We refer to this stage, in which defects are well distinguished, as the *pre-collision* regime. The approaching defects obey the scaling $d(t) \approx (t_c - t)^{0.5 \pm 0.2}$, where t_c stands for the collision time. The velocities of both defects are comparable. Note that experimentally different velocities are observed what is presumably due to the back flow effects, which we have not taken into account [14].

When $d \approx \xi_{eq}$ (approximately 2400 sweeps) the core structure of defects become influenced by each other and the "ring" radia apparently

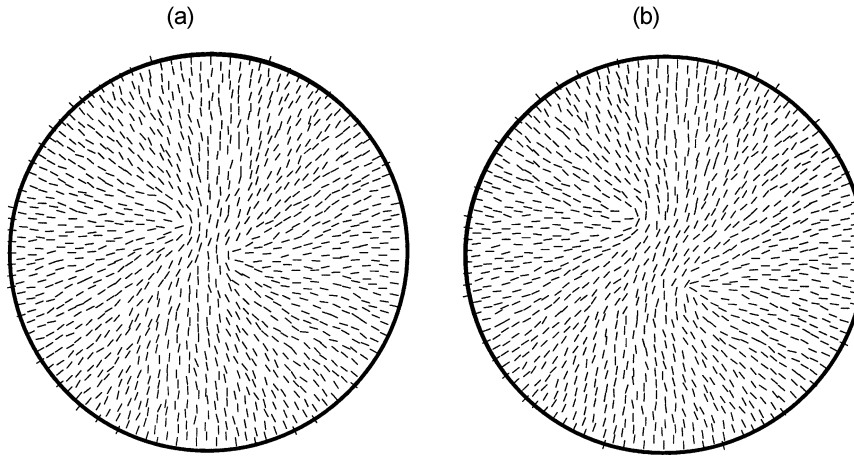

FIGURE 3 The (x,y) cross-sections indicated in Figure 2b: (a) II, (b) I or III. The cross-sections of (I) and (iii) are very similar but relatively rotated in the (x,y) plane.

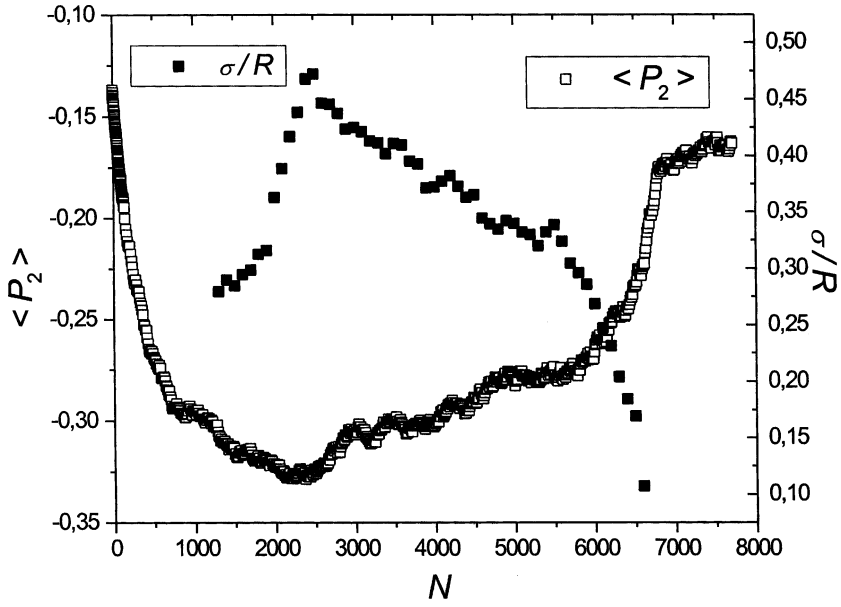

FIGURE 4 The ring radia and $\langle P_2 \rangle$ time evolution. $\sigma = 2\xi_r$ in the pre-collision regime and $\sigma = \xi_r^{(post)}$ in the collision and post-collision regime. The initial strong variation of $\langle P_2 \rangle$ till $N \approx 1000$ sweeps is connected to the formation of the ring-like structure of defect. At $N \approx 2500$ the defects collide, the rings disappear at $N \approx 6600$ and the equilibrium profile is reached at $N \approx 7500$. $N_z = 70$, $2N_r = 34$, $d_0/R = 0.74$.

increase: the collision regime is entered. The "central" ER like structure, that was necessary for the topological stability of defects, is lost and the defects merge into a single twisted (Fig. 2b, Fig. 3) "ring"-like structure, characterised by $\xi_r^{(post)}$ in the direction along the cylinder axis (Fig. 2b). With time the ring shrinks and in the mean time untwists and approaches circular profile (Fig. 2c). Finally it disappears (after 6600 sweeps) and at 7500 sweeps the defectless equilibrium ER profile is reached.

In Figure 4 we show the corresponding time evolution of "ring" radia. In the same figure the time evolution of $\langle P_2 \rangle = \langle (3\cos\theta - 1)/2 \rangle_V$ is shown, indicating the structural changes in the system. Here $\langle \ldots \rangle_V$ indicates the volume average.

IV. CONCLUSIONS

We study the annihilation of nematic monopole and antimonopole within a cylindrical tube that enforces homeotropic anchoring. We use lattice

Lebwohl-Lasher model. The dynamics of the model is followed using the Brownian Molecular Dynamics. The pre-collision, collision and post-collision regime were examined. In the first regime the cores of defects are well separated with respect to ξ and defects can be clearly distinguished. The quasi-equilibrium structure of each core is characterised by a "ring"-like structure. In this regime the interaction between defects is partially shielded by boundary conditions. When defect come sufficiently close their ring radia increase. Then "rings" collide (collision regime) and merge into a single "ring" that gradually shrinks and disappears establishing the defectless ER structure (post-collision regime).

In the simulation, consisting of approximately 10^6 particles, the annihilation of defects initially placed at a distance $d_0/(2R) \approx 0.74$ is realised in less than 10000 sweeps. The time interval corresponding to a sweep depends on the elastic and viscous properties of the nematic LC and cylinder radius [19]. Note that typical time scales of the pre-collision and post-collision regime in our simulation are comparable because ξ and R are of the same order of magnitude. One expects that the typical time scales are proportional to R^2 and ξ^2 in the pre and post-collision regime, respectively [9]. The annihilation dynamics of the first regime is governed by nematic director field and in the second regime by the nematic order parameter field.

REFERENCES

[1] Mermin, N. D. (1979). *Rev. Mod. Phys.*, *51*, 591–648.
[2] Kleman, M. (1983). *Points, Lines and Walls*. Chichester: Wiley.
[3] Schopol, N. & Sluckin, T. J. (1988). *J. Phys. (France)*, *49*, 1097–1101.
[4] Penzenstadler, E. & Trebin, H. R. (1989). *J. Phys. (France)*, *50*, 1027–1040.
[5] Rosso, R. & Virga, E. G. (1996). *J. Phys. A.*, *29*, 4247–4264.
[6] Gartland, E. C. & Mkaddem, S. (1999). *Phys. Rev. E.*, *59*, 563–567.
[7] Kralj, S., Virga, E. G., & Žumer, S. (1999). *Phys. Rev. E.*, *60*, 1858–1866; *J. Phys. A: Math. Gen.*, 2001, *34*, 829–838.
[8] Kurik, M. V. & Lavrentovich, O. D. (1988). *Sov. Phys. Usp.*, *31*, 196; (*Usp. Fiz. Nauk*, 1988. *154*, 381–431), and references therein.
[9] Virga, E. G. private communication.
[10] Pargellis, A. N., Turok, N., & Yurke, B. (1991). *Phys. Rev. Lett.*, *67*, 1570–1573.
[11] Pismen, L. M. & Rubinstein, B. Y. (1992). *Phys. Rev. Lett.*, *69*, 96–99.
[12] Peroli, G. G. & Virga, E. G. (1999). *Phys. Rev. E.*, *59*, 3027–3032.
[13] Toth, G., Denniston, C., & Yeomans, J. M. (2002). *Phys. Rev. Lett.*, *88*, 105504.
[14] Svenšek, D. & Žumer, S. to be published.
[15] Lebwohl, P. A. & Lasher, G. (1972). *Phys. Rev. A.*, *6*, 426.
[16] Chiccoli, C., Pasini, P., Semeria, F., Berggren, E., & Zannoni, C. (1996). *Mol. Cryst. Liq. Cryst.*, *290*, 237–244.
[17] Barbero, G. (1991). *Mol. Cryst. Liq. Cryst.*, *195*, 199–220.
[18] de Gennes, P. G. & Prost, J. (1993). *The Physics of Liquid Crystals*. Oxford University Press: Oxford.

[19] Bradač, Z., Kralj, S., & Žumer, S. (2002). *Phys. Rev. E.*, *58*, 7447–7454; *ibid.*, 2002, *65*, 21705.
[20] Ermak, D. L. (1975). *J. Chem. Phys.*, *62*, 4189–4196.
[21] Williams, E., Cladis, P. E., & Kleman, M. (1973). *Mol. Cryst. Liq. Cryst.*, *21*, 355–373.
[22] Crawford, G. P., Allender, D. W., & Doane, J. W. (1992). *Phys. Rev. A.*, *45*, 8693–8708.
[23] Lubensky, T. C., Pettey, D., Currier, N., & Stark, H. (1998). *Phys. Rev. E.*, *57*, 610–625.
[24] Sonnet, A. private communication.